Supporting Information

Effect of Cysteine Oxidation in SARS-CoV-2 Receptor-Binding Domain on Its Interaction With Two Cell Receptors: Insights From Atomistic Simulations

Maryam Ghasemitarei[1,2*], Angela Privat-Maldonado[2], Maksudbek Yusupov[2,3], Shadi Rahnama[4], Annemie Bogaerts[2], Mohammad Reza Ejtehadi[1*]

[1]Department of Physics, Sharif University of Technology, Tehran 14588-89694, Iran

[2]Research Group PLASMANT, Department of Chemistry, University of Antwerp, Universiteitsplein 1, B-2610, Antwerp, Belgium

[3]Laboratory of Thermal Physics of Multiphase Systems, Arifov Institute of Ion-Plasma and Laser Technologies, Academy of Sciences of Uzbekistan, Durmon yuli str. 33, 100125, Tashkent, Uzbekistan

[4]Institute for Nanoscience & Nanotechnology (INST), Sharif University of Technology, Azadi Avenue, P.O. Code: 14588-89694,Tehran, IRAN

Oxidation of amino acids

Takai et al. [1] studied the chemical alteration of amino acids upon oxidation, using cold atmospheric plasma (CAP) as an external source of reactive oxygen and nitrogen species (RONS) that are responsible for oxidation. After CAP treatment, the chemical modification of 14 out of 20 amino acids was observed using high-resolution mass spectrometry. The oxidation of the electron-rich groups in the side chain of amino acids caused by CAP-induced reactive species could generate various types of products

Table S1. Amino acids that are most susceptible to oxidation (adopted from [2]).

Amino acids	Oxidation product
Cysteine (Cys)	Disulfides, cysteic acid
Methionine (Met)	Methionine sulfoxide, methionine sulfone
Tryptophan (Trp)	2-, 4-, 5-, 6-, and 7-Hydroxytryptophan, nitrotryptophan, kynurenine, 3-hydroxykynurinine, formylkynurinine
Phenylalanine (Phe)	2,3-Dihydroxyphenylalanine, 2-, 3-, and 4-hydroxyphenylalanine
Tyrosine (Tyr)	3,4-Dihydroxyphenylalanine, tyrosine-tyrosine cross-linkages, Tyr-O-Tyr, cross-linked nitrotyrosine
Histidine (His)	2-Oxohistidine, asparagine, aspartic acid
Arginine (Arg)	Glutamic semialdehyde
Lysine (Lys)	a-Aminoadipic semialdehyde

Proline (Pro)	2-Pyrrolidone, 4- and 5-hydroxyproline pyroglutamic acid, glutamic semialdehyde
Threonine (Thr)	2-Amino-3-ketobutyric acid
Glutamyl (Glu)	Oxalic acid, pyruvic acid

Formation of cystine and sulfonation of thiol groups in Cys, sulfoxidation of Met, hydroxylation and nitration of aromatic rings in Tyr, Phe and Trp, amidation and ring opening in His and Pro, as well as no oxidation in other six amino acids (Gly, Ser, Thr, Asn, and Asp) has been observed after CAP treatment [1]. Their investigations on 20 amino acids revealed that the reactivity of amino acids to CAP treatment is the highest for Met and Cys, whereas Trp, Phe, Tyr and the others come next in order. The same conclusions were made by Zhou et al. [3]. They observed that the relative reactivity of CAP-treated amino acids come in descending order as follows: sulfur containing (Met and Cys) > aromatic (Trp, Phe and Tyr) > five-membered ring (His and Pro) > other amino acids. Notably, in both studies Met was completely degraded after 10 min of CAP treatment, whereas about half of Cys was oxidized to its final product in this period of time [1, 3]. As Met and Cys are highly reactive amino acids, it is most likely that they are primarily oxidized by CAP.

Computational details

Figure S1 illustrates the root mean square deviation (RMSD) of four replicas of the native and oxidized RBD-ACE2 complexes. It is clear that all four replicas of the native RBD-ACE2 system reached their equilibrated state after 50 ns simulation (Figure S1A). For the oxidized RBD-ACE2 system, the MD simulations were extended up to 310 ns to ensure that all four replicas were well equilibrated. The RMSD results revealed that all replicas were almost equilibrated after 100 ns (see Figure S1B). However, the RMSD of individual RBD (Figure S2) in the oxidized RBD-ACE2 system showed that this protein was not equilibrated yet after 100 ns. Therefore, we extended the simulation time up to 300 ns. As is clear from Figure S1, the final RMSD values were obtained to be fluctuating around 0.35 nm for both the native and oxidized RBD-ACE2 complexes.

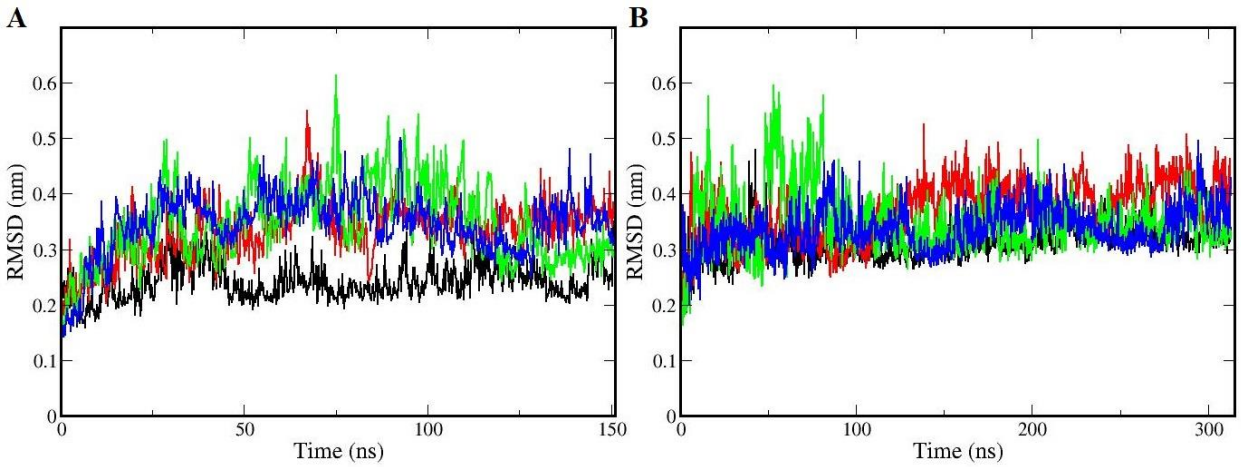

Figure S1. RMSD of four replicas of the native (A) and oxidized (B) RBD-ACE2 complexes. All replicas reach their equilibration after 50 ns and 200 ns, for the native and oxidized RBD-ACE2 complexes, respectively.

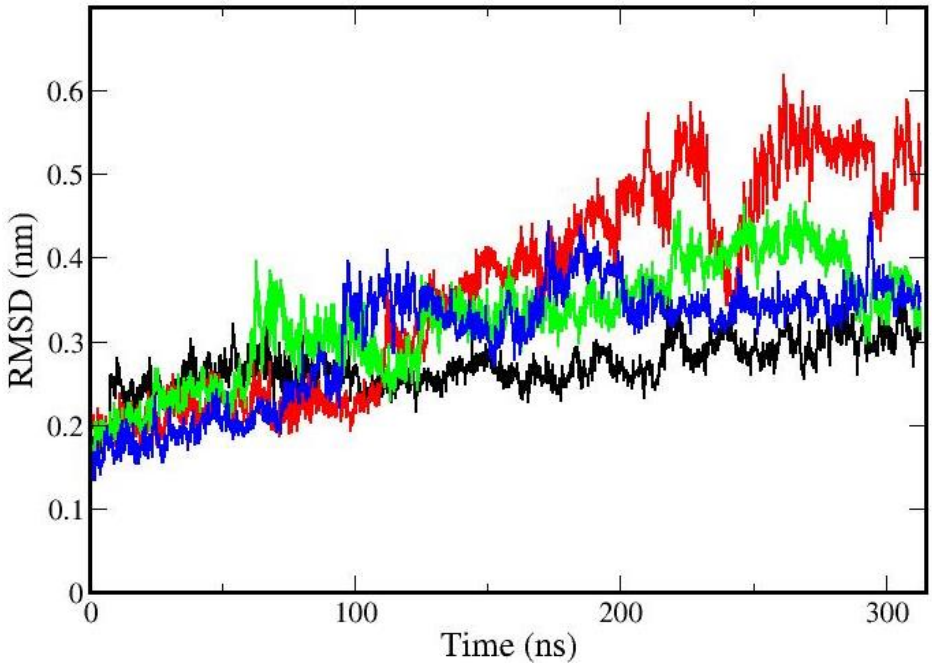

Figure S2. RMSD of four replicas of the RBD in the oxidized RBD-ACE2 complex. All replicas reach their equilibration after 250 ns.

Figure S3 illustrates the RMSD of three replicas of the native RBD-GRP78 system and its separate fragments RBD and GRP78. Initial structures (replicas) of this system were extracted from the molecular

docking and then equilibrated using the MD simulations. It is clear that the RMSD of replica-2 (red) fluctuates around 0.7 nm, which is lower than the RMSDs of replica-1 (~1 nm) and replica-3 (~2 nm).

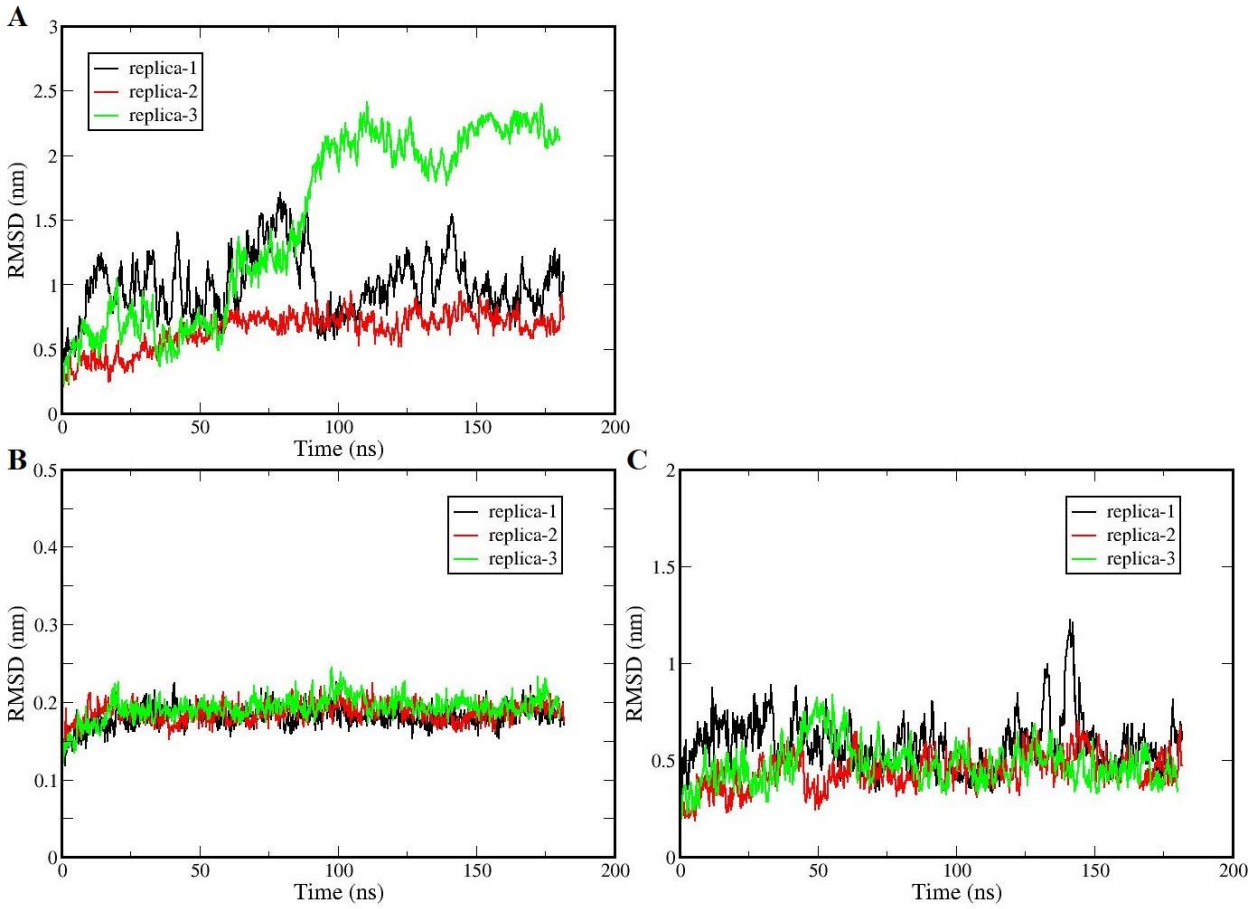

Figure S3. RMSD of three replicas of the native RBD-GRP78 complex (A), and its separate fragments RBD (B) and GRP78 (C). All replicas reach their equilibration after 100 ns. The initial structures (replicas) of the native RBD-GRP78 complex were extracted from the molecular docking simulations and then equilibrated applying MD simulations.

After choosing replica-2 as initial structure for the native and oxidized RBD-GRP78 complex, we created four new replica structures for both of them and equilibrated them using different initial velocities of the atoms, in order to ensure that all four structures of each system are consistent. From all four replicas of the oxidized RBD-GRP78 complex, in one case, GRP78 and RBD were separated from each other. Therefore, the RMSDs of the RBD-GRP78 structure were calculated over the other three replicas. The RMSD results of the native and oxidized RBD-GRP78 complexes revealed that all replicas were almost equilibrated after 150 ns (Figure S4). The final RMSDs were obtained to be fluctuating at around 0.5 nm and 1.5 nm for the native and oxidized RBD-GRP78 complexes, respectively.

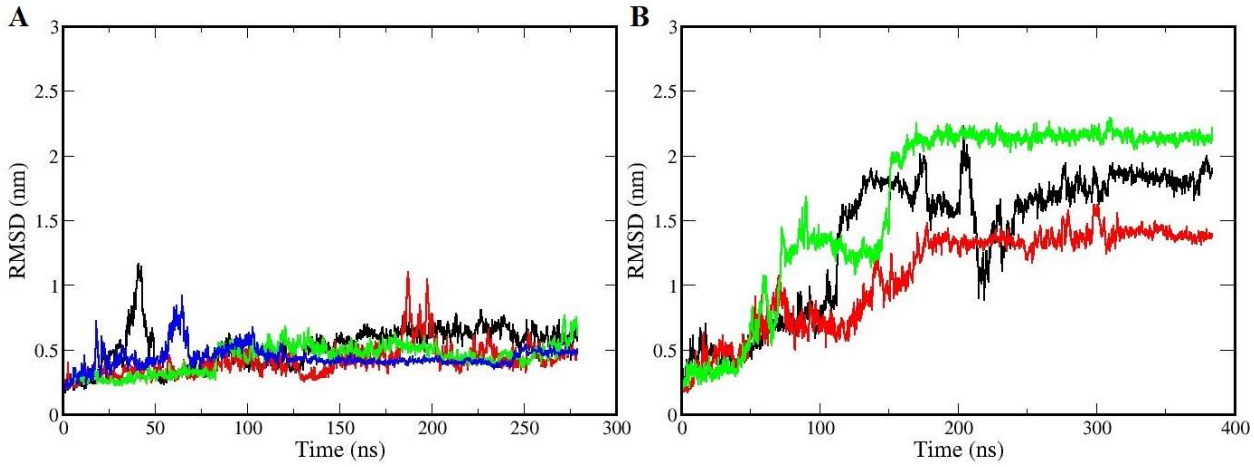

Figure S4. RMSD of the native (A) and oxidized (B) RBD-GRP78 system for all replicas. All replicas reach their equilibration after 150 ns and 200 ns, for the native and oxidized RBD-GRP78 complexes, respectively.

Figure S5 represents the averaged root mean square fluctuation (RMSF) of amino acid residues of the RBD and ACE2 proteins in the native (green) and oxidized (red) RBD-ACE2 complexes. The results showed that the oxidation of Cys residues to cysteic acids (CYOs) in the RBD increases the fluctuation of amino acid residues located around them, indicating the separation of these residues from other parts of the RBD, as well as from the interface with ACE2.

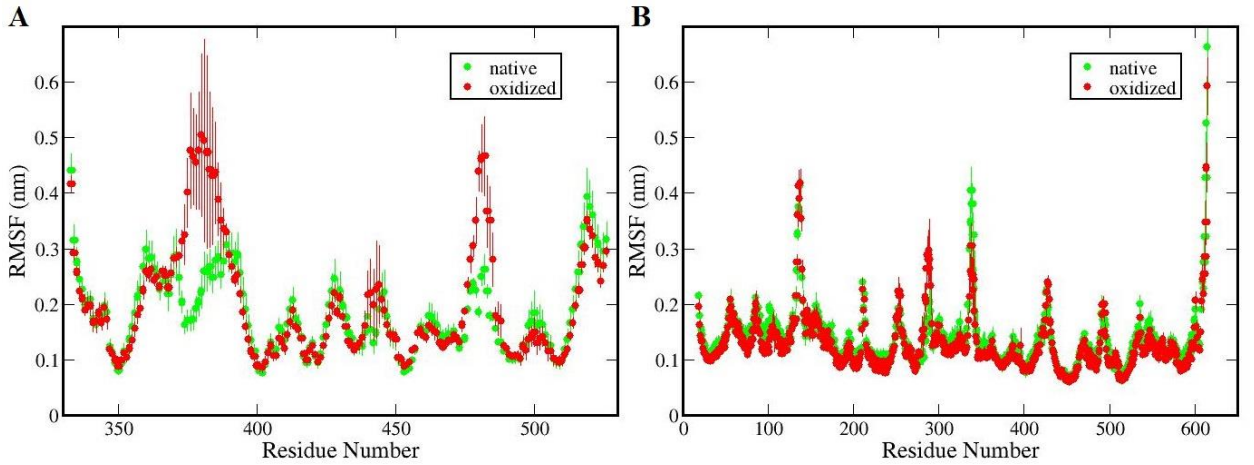

Figure S5. RMSF of amino acid residues of the RBD (A) and ACE2 (B) in the native (green) and oxidized (red) RBD-ACE2 complexes. The results are obtained from the last 100 ns of the MD simulations and averaged over four replicas.

Table S2 and S3 show the number of most probable H-bonds and salt bridges between amino acid residues of the RBD and ACE2, with the abundance of more than 10%, in the native and oxidized complexes, respectively.

Table S2. Number of H-bonds and salt bridges formed between residues of the native RBD and ACE2 proteins. The values are obtained by dividing the total number of H-bonds (or salt bridges) to the total number of MD frames (with the abundance of more than 10% in all frames), using the last 100 ns of the MD simulation.

region of RBD	native RBD-ACE2	number of H-bonds	number of salt bridges
II&III	Lys_{417}-Asp_{30}	0.50 ± 0.01	0.80 ± 0.06
III*	Gly_{502}-Lys_{353}	0.37 ± 0.03	-
	Thr_{500}-Asp_{335}	0.35 ± 0.09	-
	Ala_{475}-Ser_{19}	0.13 ± 0.03	-
IV	Asn_{487}-Tyr_{83}	0.32 ± 0.02	-
	Glu_{484}-Lys_{31}	0.21 ± 0.05	0.32 ± 0.08

Table S3. Number of H-bonds and salt bridges formed between residues of the oxidized RBD and ACE2 proteins. The values are obtained in the same way as mentioned in Table S1.

region of RBD	oxidized RBD-ACE2	number of H-bonds	number of salt-bridges
II&III	Lys_{417}-Asp_{30}	0.38 ± 0.05	0.89 ± 0.06
III*	Gly_{502}-Lys_{353}	0.38 ± 0.05	-
	Thr_{500}-Asp_{355}	0.34 ± 0.08	-
	Gln_{498}-Lys_{353}	0.18 ± 0.10	-
	Gln_{493}-Glu_{35}	0.15 ± 0.05	-
	Tyr_{505}-Glu_{37}	0.13 ± 0.06	-
	Gly_{496}-Lys_{353}	0.11 ± 0.05	-

Figure S6 represents the averaged RMSF of amino acid residues of the RBD and GRP78 proteins in the native (green) and oxidized (red) RBD-GRP78 complexes. The results indicate that oxidation of Cys residues to CYOs in RBD increases the fluctuation of all amino acid residues of the RBD located around CYO residues (Figure S6A), as well as some amino acid residues of the GRP78 (Figure S6B), indicating the separation of RBD and GRP78 from each other.

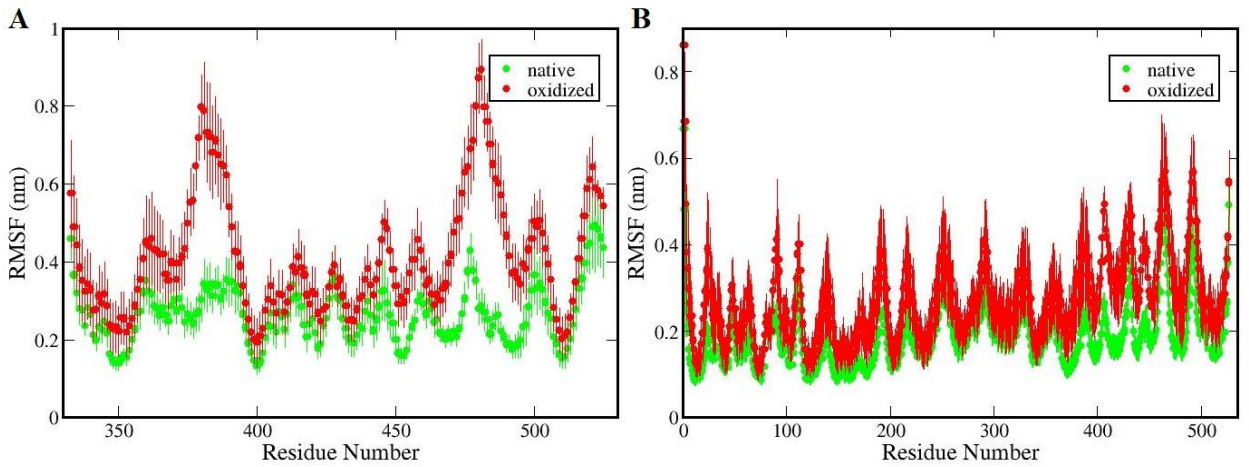

Figure S3. RMSF of amino acid residues of the RBD (A) and GRP78 (B) in the native (green) and oxidized (red) RBD-GRP78 complexes. The results are obtained from the last 100 ns of the MD simulations and averaged over four (native) and three (oxidized) replicas.

Table S4 and S5 show the number of most probable H-bonds and salt bridges between amino acid residues of the RBD and GRP78, with the abundance of more than 10%, in the native and oxidized complexes, respectively.

Table S4. Number of H-bonds and salt bridges formed between residues of the native RBD and GRP78 proteins. The values are obtained in the same way as mentioned in Table S1.

region of RBD	native RBD-GRP78	number of H-bonds	number of salt bridges
III*	Tyr_{505}-Glu_{220}	0.15 ± 0.10	-
	Gly_{477}-Pro_{421}	0.12 ± 0.08	-
IV	Glu_{484}-Lys_{412}	0.24 ± 0.05	0.16 ± 0.14
	Glu_{484}-Lys_{424}	0.21 ± 0.09	0.42 ± 0.18
	Glu_{484}-Thr_{411}	0.17 ± 0.04	-

Table S5. Number of H-bonds and salt bridges formed between residues of the oxidized RBD and GRP78 protein. The values are obtained in the same way as mentioned in Table S1.

region of RBD	oxidized RBD-GRP78	number of H-bonds	number of salt bridges
I	Glu_{340}-Lys_{140}	0.17 ± 0.11	0.29 ± 0.08
III*	Arg_{466}-Asp_{3}	0.29 ± 0.21	-
	Lys_{444}-Asp_{390}	0.12 ± 0.09	0.20 ± 0.09

1. Takai, E.; Kitamura, T.; Kuwabara, J.; Ikawa, S.; Yoshizawa, S.; Shiraki, K.; Kawasaki, H.; Arakawa, R.; Kitano, K., Chemical modification of amino acids by atmospheric-pressure cold plasma in aqueous solution. *Journal of Physics D: Applied Physics* **2014,** *47* (28), 285403.
2. Berlett, B. S.; Stadtman, E. R., Protein oxidation in aging, disease, and oxidative stress. *Journal of Biological Chemistry* **1997,** *272* (33), 20313-20316.
3. Zhou, R.; Zhou, R.; Zhuang, J.; Zong, Z.; Zhang, X.; Liu, D.; Bazaka, K.; Ostrikov, K., Interaction of Atmospheric-Pressure Air Microplasmas with Amino Acids as Fundamental Processes in Aqueous Solution. *PLOS ONE* **2016,** *11* (5), e0155584.